Progress In Electromagnetics Research C, Vol. 48, 37–44, 2014

Planar Bandpass Filter with 100-dB Suppression up to Tenfold Passband Frequency

Boris A. Belyaev[1, 2, 3, *], Alexey M. Serzhantov[1, 2], Vladimir V. Tyurnev[1, 2], Yaroslav F. Bal'va[1, 3], and Aleksandr A. Leksikov[1, 2, 3]

Abstract—This paper proposes a miniature microwave bandpass filter. It comprises quasi-lumped suspended substrate stripline resonators of a new type. Their common substrate consists of two contiguous dielectric layers. Every resonator in the filter has three parallel strip conductors. Two of them are placed on the outer substrate surfaces and the rest is placed inside the substrate. The filter of the sixth order was designed with the use of special optimization rules that are universal for all resonator filters. The substrate of the fabricated filter was made of RT/Duroid 5880 ($\varepsilon_r = 2.2$, $\tan\delta = 0.002$) with thickness of 0.127 mm. It has dimensions of 12 mm × 45.5 mm. The measured passband has a center frequency of 1.01 GHz, 3-dB fractional bandwidth of 11%, and minimum insertion loss of 1.4 dB. The 100-dB upper stopband extends up to 10.5 GHz.

1. INTRODUCTION

All bandpass resonator filters have spurious passbands at resonant frequencies of higher modes of their resonators. These passbands limit the width of the upper stopband and/or weaken rejection in the latter, that is, they make filter selectivity worse. One of the methods for stopband widening is the use of stepped-impedance resonators. Stopband width in this case increases with increasing impedance step [1, 2]. However, this increase is accompanied by significant decay of resonator unloaded Q factor resulting in increase of insertion loss. For suppression of the spurious passbands, dissimilar stepped-impedance resonators with differing frequencies of high-order modes may be used [3]. One of the spurious passbands can be suppressed with transmission zeros that arise when the input and output resonators are tapped to the filter ports [1, 4, 5]. Another way to widen the stopband width is nullification of the coupling between some adjacent resonators at one of the high-order mode frequencies [1, 5]. This is possible when the inductive and capacitive interactions between the resonators cancel each other, for example, at specific coupling length [6–8].

The methods mentioned enable the upper edge of the stopband to move up at the level of −60 dB not farther than $8f_0$, where f_0 is the passband center frequency. The further widening of the stopband needs the development of new structures of resonators with the second mode frequency many times higher than the first mode frequency. For example, a fourth-order filter based on novel coaxial resonators [9] has the upper stopband at the level of −90 dB which extends up to $47f_0$ [10]. However, from the point of view of manufacturability, reliability, and cost, such filters are significantly worse than constructions based on stripline or microstrip structures.

In this paper, we first studied resonant properties of a novel quasi-lumped planar resonator [11, 12]. This study together with use of physical optimization rules [13, 14] has allowed us to design a bandpass filter of the sixth order with wide and deep upper stopband.

Received 30 January 2014, Accepted 26 February 2014, Scheduled 4 March 2014

* Corresponding author: Boris A. Belyaev (belyaev@iph.krasn.ru).

[1] Kirensky Institute of Physics, Siberian Branch, Russian Academy of Sciences, Krasnoyarsk 660036, Russia. [2] Institute of Engineering Physics and Radio Electronics, Siberian Federal University, Krasnoyarsk 660074, Russia. [3] Reshetnev Siberian State Aerospace University, Krasnoyarsk 660014, Russia.

2. PLANAR THREE-CONDUCTOR RESONATOR

The quasi-lumped planar three-conductor resonator may be used as both a suspended stripline construction and a monolithic LTCC construction. Figure 1 shows the longitudinal section of the suspended stripline resonator. It consists of a double-layer suspended substrate and three parallel strip conductors. Two outer conductors are connected by one of their ends to one of the sidewalls of the metal shielding case. The third conductor is connected by one of its ends to the opposite sidewall. All other ends of the strip conductors do not reach the sidewalls and remain open circuited.

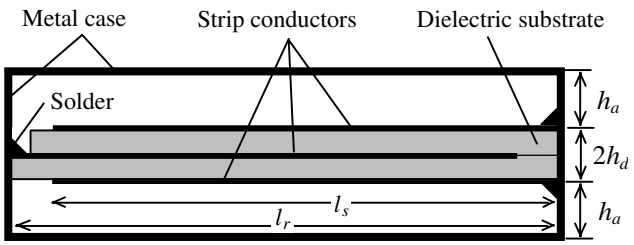

Figure 1. Longitudinal section of the suspended stripline resonator.

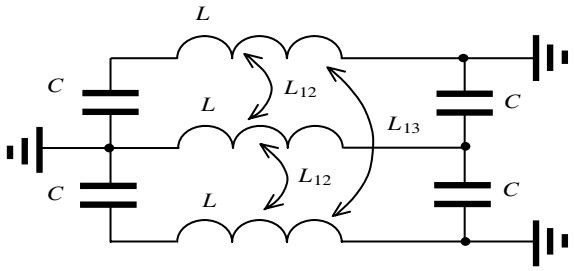

Figure 2. Simplified equivalent circuit of the resonator.

Each of the first three lower oscillation modes of the resonator, as opposed to all other modes, has only one voltage node located at the grounded end for each strip conductor. These three modes may be approximately simulated with the equivalent circuit shown at Figure 2. Solving Kirchhoff's equations for the equivalent circuit one can get the following formulas for the resonant frequencies.

$$f_1 = \frac{1}{2\pi}\sqrt{\frac{3L + L_{13} - \sqrt{(L - L_{13})^2 + 16L_{12}^2}}{4C\left(L^2 + LL_{13} - 2L_{12}^2\right)}}, \tag{1}$$

$$f_2 = \frac{1}{2\pi}\frac{1}{\sqrt{C\left(L - L_{13}\right)}}, \tag{2}$$

$$f_3 = \frac{1}{2\pi}\sqrt{\frac{3L + L_{13} + \sqrt{(L - L_{13})^2 + 16L_{12}^2}}{4C\left(L^2 + LL_{13} - 2L_{12}^2\right)}}. \tag{3}$$

Here, frequency f_1 corresponds to the first mode. Its currents in all three conductors flow in the same direction.

Frequency f_2 corresponds to the second mode. Its currents in the upper and lower conductors flow in opposite directions while the current in the inner conductor does not flow. That is why frequency f_2 does not depend on the mutual inductance L_{12}. An important peculiarity of the second mode is zero voltage along the inner strip conductor in the resonator.

Frequency f_3 corresponds to the third mode. For this mode, the currents in the upper and lower conductors flow in the same direction and the current in the inner conductor flows in the opposite direction.

Our estimation for (1) shows that $f_1 < f_2 < f_3$, so the frequency f_1 is chosen as the operating frequency in the filter. Because the second mode has zero voltage along the inner strip conductor it cannot be excited with the use of the tap made in that conductor. Therefore, the first spurious passband in the filter is generated by the third mode and frequency f_3 may set the upper edge of the stopband.

Note that the equivalent circuit in Figure 2 and formula (1) are not intended for designing resonators or filters. They just help us to classify three lower modes of the resonator by their microwave field structures in order to choose an optimal way for exciting the fundamental mode.

Below, we provide the results of 3D EM simulation with the use of CST Microwave Studio®. They uncover potentialities of the resonator. Figure 3 shows the dependences of the resonant frequencies

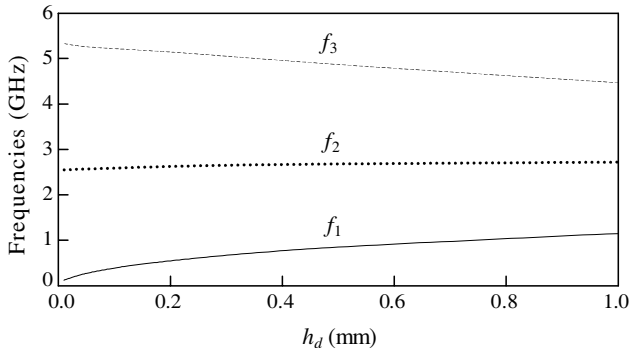

Figure 3. Resonant frequencies versus thickness of the substrate layers.

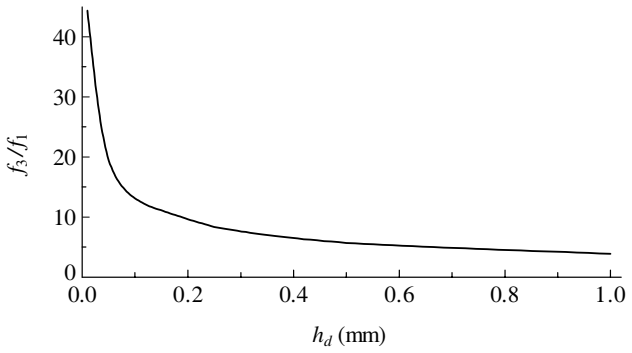

Figure 4. Frequency ratio versus thickness of the substrate layers.

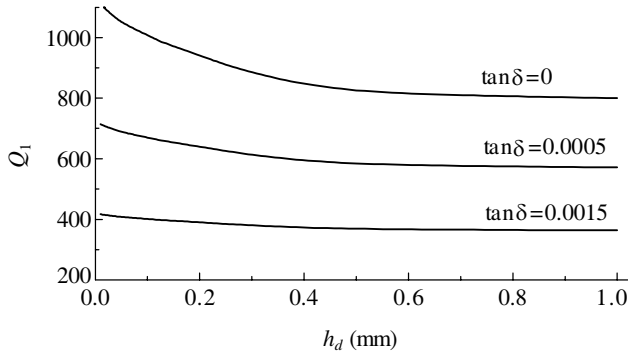

Figure 5. Unloaded quality factor versus thickness of the substrate layers at $f_1 = 1\,\text{GHz}$.

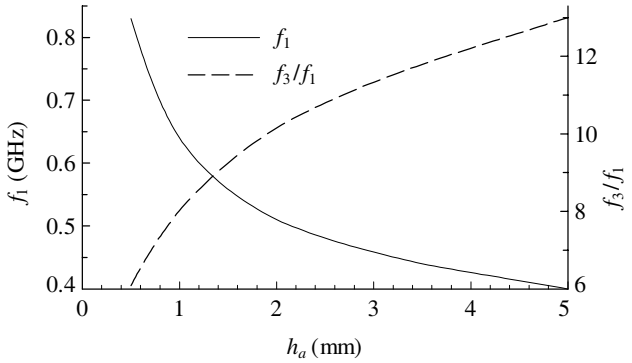

Figure 6. Resonant frequency and frequency ratio versus the air gap.

on the thickness of the substrate layers where the following parameters were used: $l_r = 20\,\text{mm}$, $h_a = 3.5\,\text{mm}$, conductor width $w = 3\,\text{mm}$, and substrate permittivity $\varepsilon_r = 2.2$.

Figure 4 shows the dependence of the frequency ratio f_3/f_1 on the thickness h_d. It was computed for the same values of l_r, h_a, w, and ε_r.

Figure 5 shows the dependences of the unloaded quality factor of the first resonance Q_1 on the thickness h_d for three values of dielectric loss tangent $\tan\delta$. They were computed for conductivity $\sigma = 5.88 \cdot 10^7\,\text{S/m}$ (copper) and the same values of h_a, w, and ε_r. The resonator length l_r was varied together with h_d in order to keep the equality $f_1 = 1\,\text{GHz}$.

All graphs in Figure 3 through Figure 5 show that a thinner h_d improves the filter performance. However, we should keep in mind that in all above 3D simulations, we supposed that thickness h_d was much greater than the skin depth.

Figure 6 shows the dependences of frequency f_1 and ratio f_3/f_1 on the air gap h_a. The simulations were carried out for $l_r = 20\,\text{mm}$, $w = 3\,\text{mm}$, $h_d = 0.127\,\text{mm}$, $\varepsilon_r = 2.2$.

Figure 7 shows the dependences of frequency f_1 and ratio f_3/f_1 on the strip width w. The simulations were carried out for $l_r = 20\,\text{mm}$, $h_d = 0.127\,\text{mm}$, $h_a = 3.5\,\text{mm}$, $\varepsilon_r = 2.2$.

Figure 8 shows the dependences of f_1 and f_3/f_1 on the substrate permittivity. The simulations were carried out for $l_r = 20\,\text{mm}$, $h_d = 0.127\,\text{mm}$, $h_a = 3.5\,\text{mm}$, $w = 3\,\text{mm}$.

Figure 9 shows the dependences of f_1 and f_3/f_1 on the normalized strip conductor length l_s/l_r. The simulations were carried out for $l_r = 20\,\text{mm}$, $h_d = 0.127\,\text{mm}$, $h_a = 3.5\,\text{mm}$, $w = 3\,\text{mm}$, $\varepsilon_r = 2.2$.

Graphs in Figure 3 through Figure 9 allow designing the resonator with optimal combination of its characteristics such as size, quality factor, and frequency ratio f_3/f_1.

This study also shows that such advantages as high values of f_3/f_1 and Q_1 remain in a case of the resonator with homogeneous dielectric filling. Therefore, monolithic LTCC technology is also suitable for implementation of the considered planar resonator.

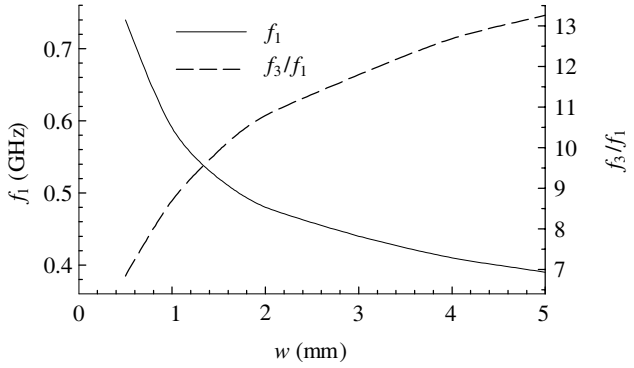

Figure 7. Resonant frequency and frequency ratio versus the strip width.

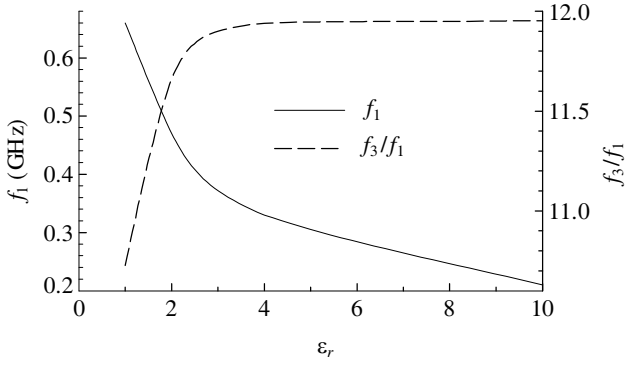

Figure 8. Resonant frequency and frequency ratio versus the permittivity.

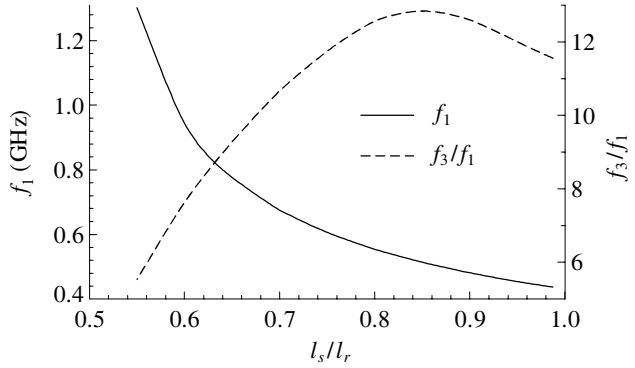

Figure 9. Resonant frequency and frequency ratio versus the normalized length.

3. FILTER DESIGN

Below, we describe the filter design for the case when the device has six resonators because it can be easily generalized for any number of resonators.

The considered layout of the suspended double-layer substrate stripline bandpass filter of the sixth order is shown in Figure 10. The filter has six parallel coupled three-conductor resonators. Two taps that are made in the inner strip conductors of the input and output resonators are the filter ports.

During the filter design, we did not use any filter prototypes, equivalent circuits, coupling coefficients or coupling matrices of resonators. Instead of those, we manually applied a special filter optimization together with 3D EM simulation. This optimization is based on the "physical rules". These rules are universal for all resonator bandpass filters [13, 14]. They are successfully used in the filter expert system *Filtex32* [15]. The efficiency of the optimization method based on the "physical rules" is several orders higher than the efficiency of any standard universal optimization method. Such comparison for sixth order microstrip bandpass filters was carried out in [16].

As is known that in order to obtain a required passband, every resonator in a bandpass filter should have optimal couplings and tuned resonant frequency. Since the filter structure is symmetrical, we have to select at least seven adjustable structure parameters, where four of them are responsible for one external and three internal couplings and the other three are responsible for resonant frequencies. All other parameters may have arbitrary values in some reasonable limits and remain fixed during the filter adjustment.

As for the coupling adjustable parameters, we chose the distance t from the port tap to the open circuited strip end and the spacings between resonators S_1, S_2, and S_3 (Figure 10).

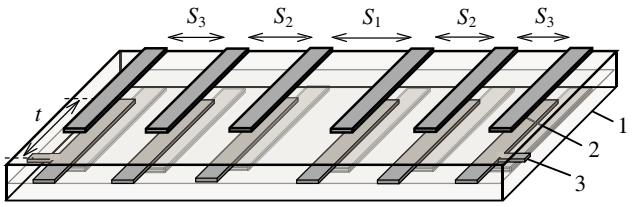

Figure 10. Layout of the suspended stripline bandpass filter; 1 — double-layer dielectric substrate, 2 — strip conductor, 3 — port.

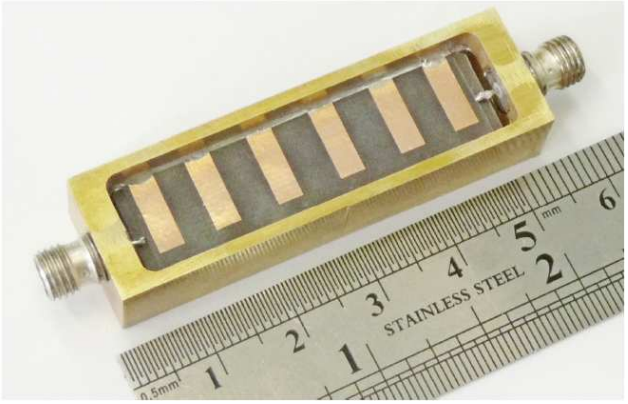

Figure 11. Photograph of the fabricated suspended stripline bandpass filter with top lid removed.

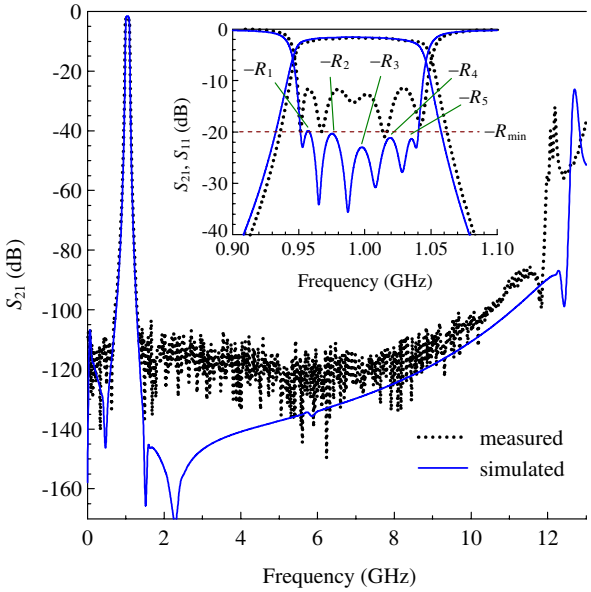

Figure 12. Frequency response of the suspended stripline bandpass filter.

As for the frequency tuning parameter, we chose first of all the strip length l_s. The two other chosen parameters are the shortcuts Δl_1 and Δl_2 of the inner strip conductor for the internal resonators. As for the external (i.e., input/output) resonators, their every strip conductor has the same length l_s. The shortcuts Δl_1 and Δl_2 are intended to equalize the inequality of the resonant frequencies caused by a different perturbation action of such resonator ambient as the neighbor wall of the metal case, the neighbor resonator or the port tap.

We characterized the current passband of the filter being tuned by seven parameters. The first two parameters are the center frequency f_c and bandwidth Δf_c. The rest of the parameters are values of return loss minima R_1, R_2, R_3, R_4, and R_5 that are situated in the passband between the six reflection minima (Figure 12). Here, the subscripts enumerate the minima from lower to higher frequency. Thus, the number of the passband parameters is equal to the number of adjustable parameters.

The goal of our optimization is to obtain only the required values of f_c and Δf_c at equalized passband ripple. The latter means that equality $R_1 = R_2 = R_3 = R_4 = R_5 = R_{\min}$ is true where $R_{\min}$ is the required return loss minimum.

The adjustable parameters in the "rule optimization" may have practically any reasonable initial values. Nevertheless, a proper choice of the initial values would facilitate and speed up the filter adjustment. The initial value for the length l_s may be equal to $\lambda_g/4$ or less where λ_g is the length of TEM wave in dielectric. The initial values for the shortcuts Δl_1 and Δl_2 may be zero. The values for the spacings S_1, S_2, and S_3 may be equal to the thickness h_a. The value for the tap distance t may be equal to $l_s/2$.

As is well-known, the passband center frequency f_c can be easily tuned in the filter by adjusting the length l_s. The bandwidth Δf_c can be tuned by simultaneous proportional variation of all the spacings S_1, S_2, and S_3. Moving the average value R_a for all the minima R_1, R_2, R_3, R_4, and R_5 toward the level $R_{\min}$ requires, first of all, varying the distance t.

Equalizing the reflection ripple in the passband is the more difficult part of the optimization. Before applying the "physical rules," the current distortion of the ripple should be expanded in the sum of normal orthogonal distortions. Every normal distortion is expressed through the values $R_1 - R_{\min}$, $R_2 - R_{\min}$, $R_3 - R_{\min}$, $R_4 - R_{\min}$, and $R_5 - R_{\min}$. There are two types of the normal orthogonal distortions. We call them even and odd. The return loss minima for any even normal distortion are bounded by the equalities

$$R_1 = R_5, \quad R_2 = R_4. \tag{4}$$

Those minima for odd normal distortion are bounded by the equalities

$$R_1 + R_5 = 2R_{\min}, \quad R_2 + R_4 = 2R_{\min}. \tag{5}$$

Any even normal distortion we eliminate by a proper correction of the coupling proportion which is determined by the spacing proportion $S_1 : S_2 : S_3$. Any odd normal distortion we eliminate by a proper correction of the detuned resonant frequencies, that is, we vary the shortcuts Δl_1 and Δl_2. Formulas for the ripple distortions together with the appropriate rules for their elimination are published in [13] for the fourth order filters, and in [14] for the sixth order filters.

Note that the spacings S_1, S_2, and S_3 in the filter with equalized transmission ripple always satisfy the inequality $S_3 < S_2 < S_1$.

We have designed the filter on the substrate of RT/Duroid 5880 with $h_d = 0.127\,\text{mm}$, $\varepsilon_r = 2.2$, and $\tan\delta \approx 0.002$. Here, the passband is to have the center frequency $f_0 = 1\,\text{GHz}$, the 3-dB fractional bandwidth $\Delta f/f_0 = 10\%$, and the minimum return loss $R_{\min} = 20\,\text{dB}$. Choosing $h_a = 3.5\,\text{mm}$, $w = 3\,\text{mm}$, and $l_s/l_r = 0.75$, we have obtained $l_r = 12\,\text{mm}$, $l_s = 9\,\text{mm}$, $\Delta l_1 = 0.33\,\text{mm}$, $\Delta l_2 = 0.31\,\text{mm}$, $t = 4.25\,\text{mm}$, $S_1 = 4.625\,\text{mm}$, $S_2 = 4.5\,\text{mm}$, and $S_3 = 3.75\,\text{mm}$. One can ascertain that $l_r = 0.059\lambda_g$. This allows us to call the three-conductor resonator as a quasi-lumped one.

4. EXPERIMENTAL AND SIMULATION RESULTS

Figure 11 shows the photograph of the fabricated filter. The double-layer substrate of the filter was made of two separate sheets of RT/Duroid 5880 with etched strip conductors on both surfaces. The strip conductors placed on one surface in each substrate were tined and properly combined. Then the sheets were pressed together and heated, and in this way, the inner conductors were formed. Thus, every inner strip conductor consists of two soldered parts.

The substrate has dimensions $12\,\text{mm} \times 45.5\,\text{mm}$. It is suspended inside the metal case with help of lugs made in its sidewalls.

Figure 12 shows the frequency response of the fabricated filter. The measured passband has the center frequency $f_0 = 1.01\,\text{GHz}$, the 3-dB fractional bandwidth $\Delta f/f_0 = 11\%$, the minimum return loss $R_{\min} = 11.5\,\text{dB}$, and the minimum insertion loss $L_{\min} = 1.4\,\text{dB}$. The measured upper stopband extends up to 10.5 GHz and 12 GHz at suppression levels of $-100\,\text{dB}$ and $-85\,\text{dB}$, respectively.

The observed very high suppression in the stopband is due to the frequency dispersion of resonator couplings which rapidly decay as they move away from the center frequency. Such coupling behavior occurs in filters based on two-conductor suspended stripline resonators. It was theoretically studied in [17]. Three transmission zeros, which one can see near the passband in the simulated frequency response, are the frequencies where coupling coefficient for at least one pair of neighbor resonators spaced by S_1, S_2 or S_3 vanishes.

5. CONCLUSION

Using 3D EM simulation, we first thoroughly studied resonant properties of the quasi-lumped planar resonator that has three strip conductors. We showed that this resonator differs in small dimensions, high unloaded Q factor, and high frequency ratio for the spurious and the fundamental modes. This high performance remains for similar homogeneous resonators made with LTCC technology.

Using the special optimization based on universal "physical rules" we designed and then fabricated the suspended substrate bandpass filter of the sixth order. It has very small dimensions along with low insertion loss and extremely wide and deep stopband.

We suppose that the high suppression in the stopband is caused by frequency dispersion of resonator couplings which rapidly decay as they move away from the center frequency.

ACKNOWLEDGMENT

This work was supported by the Siberian Branch of the Russian Academy of Sciences under Integration Project No. 109 and the Ministry of Education and Science of the Russian Federation within Research engineering in Siberian Federal University.

REFERENCES

1. Chen, Y.-M., S.-F. Chang, C.-C. Chang, and T.-J. Hung, "Design of stepped-impedance combline bandpass filters with symmetric insertion-loss response and wide stopband range," *IEEE Trans. Microw. Theory Tech.*, Vol. 55, No. 10, 2191–2199, 2007.
2. Belyaev, B. A., S. V. Butakov, N. V. Laletin, A. A. Leksikov, V. V. Tyurnev, and O. N. Chesnokov, "Selective features of microstrip filters based on irregular resonators," *J. Commun. Technol. Electron.*, Vol. 49, No. 11, 1308–1316, 2004.
3. Lin, S.-C., P.-H. Deng, Y.-S. Lin, C.-H. Wang, and C. H. Chen, "Wide-stopband microstrip bandpass filters using dissimilar quarter-wavelength stepped-impedance resonators," *IEEE Trans. Microw. Theory Tech.*, Vol. 54, No. 3, 1011–1017, 2006.
4. Kuo, J.-T. and E. Shih, "Microstrip stepped impedance resonator bandpass filter with an extended optimal rejection bandwidth," *IEEE Trans. Microw. Theory Tech.*, Vol. 51, No. 5, 1554–1559, 2003.
5. Kuo, T.-N., W.-C. Li, C.-H. Wang, and C. H. Chen, "Wide-stopband microstrip bandpass filters using quarter-wavelength stepped impedance resonators and bandstop embedded resonators," *IEEE Microw. Wireless Compon. Lett.*, Vol. 18, No. 6, 389–391, 2008.
6. Kuo, J.-T., S.-P. Chen, and M. Jiang, "Parallel-coupled microstrip filters with over-coupled end stages for suppression of spurious responses," *IEEE Microw. Wireless Compon. Lett.*, Vol. 13, No. 10, 440–442, 2003.
7. Sánchez-Soriano, M. Á., G. Torregrosa-Penalva, and E. Bronchalo, "Multispurious suppression in parallel-coupled line filters by means of coupling control," *IET Microw. Antennas Propag.*, Vol. 6, No. 11, 1269–1276, 2012.
8. Belyaev, B. A., N. V. Laletin, A. A. Leksikov, and A. M. Serzhantov, "Peculiarities of coupling coefficients of a regular microstrip resonator," *J. Commun. Technol. Electron.*, Vol. 48, No. 1, 31–38, 2003.
9. Belyaev, B. A., A. M. Serzhantov, V. V. Tyurnev, and A. A. Leksikov, "Miniature bandpass filter with a wide stopband up to $40f_0$," *Microwave Opt. Technol. Lett.*, Vol. 54, No. 5, 1117–1118, 2012.
10. Belyaev, B. A., A. M. Serzhantov, V. V. Tyurnev, A. A. Leksikov, and A. A. Leksikov, "Miniature coaxial resonator and related bandpass filter with ultra-wide stopband," *Tech. Phys. Lett.*, Vol. 38, No. 1, 47–50, 2012.
11. Belyaev, B. A., A. M. Serzhantov, V. V. Tyurnev, A. A. Leksikov, and Y. F. Bal'va, "Miniature bandpass microwave filter with interference suppression by more than 100 dB in a wide rejection band," *Tech. Phys. Lett.*, Vol. 39, No. 8, 690–693, 2013.

12. Belyaev, B. A., A. M. Serzhantov, V. V. Tyurnev, A. A. Leksikov, and Y. F. Bal'va, "Stripline bandpass filter with wide stopband and rejection level up to 100 dB," *Microwave Opt. Technol. Lett.*, Vol. 54, No. 12, 2866–2869, 2013.
13. Belyaev, B. A., A. A. Leksikov, A. M. Serzhantov, and V. V. Tyurnev, "Miniature suspended-substrate bandpass filter," *Progress In Electromagnetics Research C*, Vol. 15, 219–231, 2010.
14. Belyaev, B. A. and V. V. Tyurnev, "The method for microstrip filters parametric synthesis," *16th Int. Crimean Conference "Microwave and Telecommunication Technology"*, 517–519, Sevastopol, Ukraine, 2006.
15. Belyaev, B. A., S. V. Butakov, N. V. Laletin, A. A. Leksikov, and V. V. Tyurnev, "Expert system Filtex 32 for computer-aided design of bandpass microstrip filters," *15th Int. Crimean Conference "Microwave and Telecommunication Technology"*, 504–505, Sevastopol, Ukraine, 2005.
16. Tyurnev, V. V., "Efficiency comparison of the optimization methods that are used to design microwave filters," *VIIIth International Scientific and Practical Conference*, 75–76, Kiev, Ukraine, 2011.
17. Belyaev, B. A., A. M. Serzhantov, and A. A. Leksikov, "Analysis of the coupling coefficient of stripline resonators in the designs of suspended-substrate filters," *J. Commun. Technol. Electron.*, Vol. 55, No. 12, 1330–1339, 2010.